

Multiplicity and Transverse Energy Distributions in Au-Au and Pb-Pb Collisions at High Energy

Fu-Hu Liu,^{1,2,*} Dong-Hai Zhang,¹ Mai-Ying Duan,¹ and Nabil N. Abd Allah^{3,4}

¹*Institute of Modern Physics, Shanxi Teachers University, Linfen 041004, China*

²*Dept. of Science, North China University of Science and Technology, Taiyuan 030051, China*

³*Physics Dept., Faculty of Science, South Valley University, Sohag, Egypt*

⁴*Physics Dept., Faculty of Teachers, Box 1343, Al-Madina Al-Monoura, Saudi Arabia*

(Received June 24, 2003)

The multiplicity and transverse energy distributions in high-energy nucleus-nucleus collisions are described by a geometrical model, namely the participant-spectator model. The calculated results are compared and found to be in agreement with the experimental data on Au-Au collisions at the RHIC energy and Pb-Pb collisions at the SPS energy.

PACS numbers: 25.75.-q, 24.10.Pa

I. INTRODUCTION

Relativistic nucleus-nucleus collisions have been studied very intensively in recent years. Increasing the projectile and target mass numbers and incident energies increases the possibility of the formation of a new phase of matter, namely the quark-gluon plasma (QGP) [1]. The analyses of the experimental results using the high-energy heavy-ion beams of the Dubna Synchrophasotron, BNL-AGS, CERN-SPS, and BNL-RHIC have opened up a new area of interest in the field of heavy-ion interactions [2,3].

In relativistic nucleus-nucleus collisions, it is highly important for us to analyze the nuclear geometry. The overlapping part of the two nuclei in collision is called the participant and the other part is called the spectator. For the purpose of studying multiparticle production, e.g. the multiplicity and transverse energy distributions, it is useful to calculate the number of participant nucleons.

In this paper, we use the participant-spectator model [4] to explain the multiplicity and transverse energy distributions. As the first step, the number of participant nucleons are calculated. Then the multiplicity and transverse energy distributions in Au-Au and Pb-Pb collisions at high energy are obtained.

II. NUMBER OF PARTICIPANT NUCLEONS

We assume that the incoming direction of the projectile is the coordinate axis z and the reaction plane is the coordinate plane xoz ; then the reference frame fixed on the projectile is established. Let A_P and A_T denote the mass numbers of the projectile and the target, respectively, and b denote the impact parameter. At a fixed b , the nucleon numbers

in the projectile and target participants are

$$n_P = \int \rho \left(\sqrt{x^2 + y^2 + z^2} \right) \theta \left(R_P - \sqrt{x^2 + y^2 + z^2} \right) \theta \left[R_T - \sqrt{(x-b)^2 + y^2} \right] dx dy dz, \quad (1)$$

and

$$n_T = \int \rho \left[\sqrt{(x-b)^2 + y^2 + z^2} \right] \theta \left[R_T - \sqrt{(x-b)^2 + y^2 + z^2} \right] \theta \left(R_P - \sqrt{x^2 + y^2} \right) dx dy dz, \quad (2)$$

respectively, where $R_P = r_0 A_P^{1/3}$ is the projectile radius, $R_T = r_0 A_T^{1/3}$ is the target radius, and $r_0 = 1.2\text{fm}$. The parameter ρ in the equations is the Woods-Saxon shape of nucleon number density distribution [5]. For nuclei with $A_P, A_T > 16$, we have

$$\rho \left(\sqrt{x^2 + y^2 + z^2} \right) = \frac{\rho_0}{1 + \exp[(\sqrt{x^2 + y^2 + z^2} - R_P)/c]}, \quad (3)$$

and

$$\rho \left[\sqrt{(x-b)^2 + y^2 + z^2} \right] = \frac{\rho_0}{1 + \exp\{[\sqrt{(x-b)^2 + y^2 + z^2} - R_T]/c\}}, \quad (4)$$

respectively, where ρ_0 is the normalized constant and $c = 0.545\text{fm}$ [5]. If we regard the nucleon number density distribution in a heavy nucleus as an even one then $\rho = 3/(4\pi r_0^3)$. The total number of participant nucleons in both the projectile and target nuclei can be given by

$$n = n_P + n_T. \quad (5)$$

The BNL-RHIC has accelerated gold nuclei, and the CERN-SPS has accelerated lead nuclei. In order to study the multiplicity and transverse energy distributions in Au-Au and Pb-Pb collisions, Figure 1 presents the relationship between the participant nucleon number n and the impact parameter b for Au-Au collisions (lower two curves) and Pb-Pb collisions (upper two curves). The continuous curves are the results corresponding to the Woods-Saxon shape of the nucleon number density distribution in nuclei. The dashed and dotted curves are the results of the even distribution. One can see that the $n - b$ relationships corresponding to the two distributions for the same collision process are similar.

III. MULTIPLICITY DISTRIBUTION

We assume that the multiplicity (N_i) distribution contributed by the i -th nucleon in the projectile and target participants is

$$f_N(N_i) = \frac{1}{\langle N_i \rangle} \exp\left(-\frac{N_i}{\langle N_i \rangle}\right), \quad (6)$$

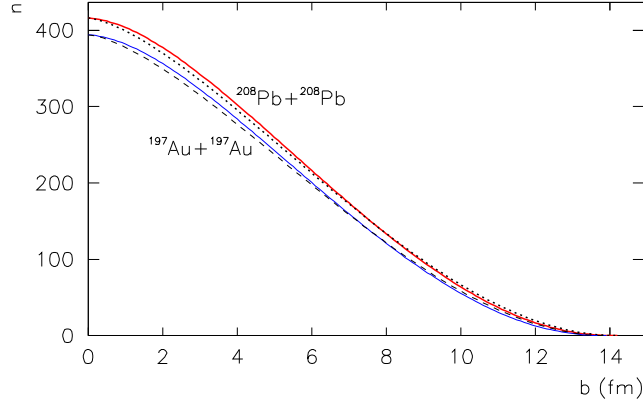


FIG. 1: Relationship between the participant nucleon number n and the impact parameter b in Au-Au and Pb-Pb collisions.

where

$$\langle N_i \rangle = \int N_i f_N(N_i) dN_i \quad (7)$$

is the mean value of the multiplicity contributed by the i -th nucleon. Then the multiplicity (N) distribution at a fixed b is given by

$$\frac{d\sigma}{dN(b)} = \sigma \int \prod_{i=1}^n f_N(N_i) \delta \left[\left(\sum_{i=1}^n N_i \right) - N \right] \prod_{i=1}^n dN_i = \frac{\sigma N^{n-1}}{(n-1)! \langle N_i \rangle^n} \exp \left(-\frac{N}{\langle N_i \rangle} \right), \quad (8)$$

where σ is the experimental cross-section measured in the final state. The distribution described by the right side of Eq. (8) is called an Erlang distribution. For comparison between the theoretical result and experimental data, we have to integrate Eq. (8) over b . Then the multiplicity distribution in the final state is

$$\frac{d\sigma}{dN} = \frac{2}{(R_P + R_T)^2} \int_0^{R_P+R_T} \frac{d\sigma}{dN(b)} db. \quad (9)$$

In the calculation of the multiplicity distribution in this paper, we use the Monte Carlo method, since Eq. (8) has a too large n to calculate $(n-1)!$ and N^{n-1} in central Au-Au and Pb-Pb collisions. According to Eq. (6), the multiplicity contributed by the i -th nucleon can be obtained by

$$N_i = -\langle N_i \rangle \ln R_i(1), \quad (10)$$

where $R_i(1)$ is a random variable distributed evenly in $[0,1]$. At a fixed impact parameter b , the multiplicity is regarded as

$$N = -\sum_{i=1}^n \langle N_i \rangle \ln R_i(1). \quad (11)$$

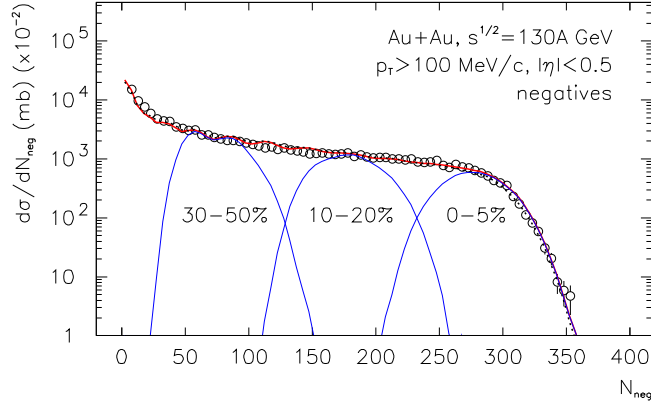


FIG. 2: Multiplicity distribution of negative charged particles produced in Au-Au collisions at $\sqrt{s} = 130A$ GeV. The circles are the experimental data quoted in Ref. [6] and the curves are our calculated results.

Considering the random selection of b , then the various n are obtained. Going one step further, the various N can be obtained. The multiplicity distribution is finally obtained by the statistical method.

Figure 2 shows the multiplicity distribution of negative charged particles produced in Au-Au collisions at $\sqrt{s} = 130A$ GeV. The circles are the experimental data quoted in Ref. [6] and the negatives with $p_T > 100$ MeV/ c and $|\eta| < 0.5$, where p_T and η denote the transverse momentum and pseudorapidity, respectively. The thick continuous and dotted curves are our calculated results, corresponding to the Woods-Saxon shape and the even nucleon number density distribution, respectively. The three thin curves are our calculated results for three different centrality cuts. In the calculation, we take $\langle N_i \rangle = 0.785$. The calculated results corresponding to both nucleon number density distributions are in agreement with the experimental data. For both calculated results, there is a little difference in the knee part. In the other parts, both calculated results are almost the same.

The multiplicity distribution of charged particles produced in Pb-Pb collisions at $158A$ GeV is given in Fig. 3. The circles are the experimental data quoted in Ref. [7] and the charged particles with $2.35 < \eta < 3.75$. The thick continuous and dotted curves are our calculated results, corresponding to the Woods-Saxon shape and even nucleon number density distribution, respectively. The three thin curves are our calculated results for three different centrality cuts. In the calculation, we take $\langle N_i \rangle = 1.780$. The calculated results corresponding to both nucleon number density distributions are in agreement with the experimental data. For both calculated results, there is a little difference in the knee part. In the other part, both calculated results are almost the same.

Figure 4 presents the multiplicity distribution of γ -like clusters produced in Pb-Pb collisions at $158A$ GeV. The circles are the experimental data quoted in Ref. [7] and the γ -like clusters with $2.8 < \eta < 4.4$. The thick continuous and dotted curves are our calcu-

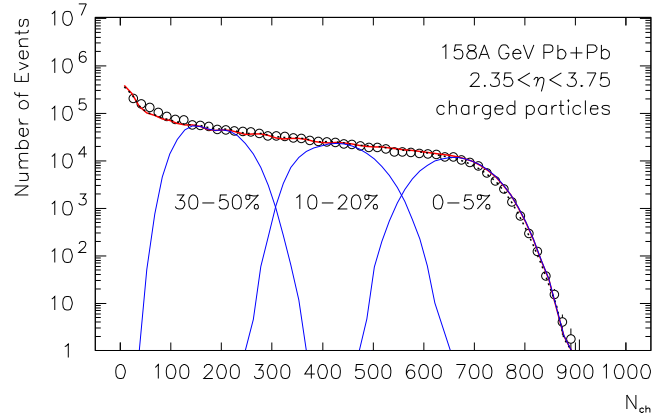


FIG. 3: Multiplicity distribution of charged particles produced in Pb-Pb collisions at 158A GeV. The circles are the experimental data quoted in Ref. [7] and the curves are our calculated results.

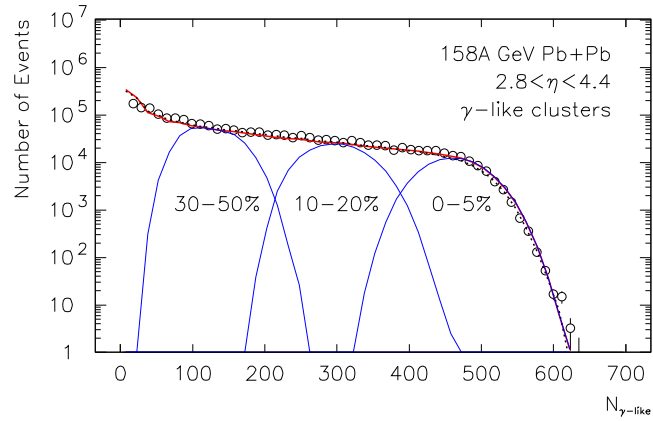


FIG. 4: Multiplicity distribution of γ -like clusters produced in Pb-Pb collisions at 158A GeV. The circles are the experimental data quoted in Ref. [7] and the curves are our calculated results.

lated results, corresponding to the Woods-Saxon shape and even nucleon number density distribution, respectively. The three thin curves are our calculated results for three different centrality cuts. In the calculation, we take $\langle N_i \rangle = 1.242$. The calculated results corresponding to both nucleon number density distributions are in agreement with the experimental data. For both calculated results, there is a little difference in the knee part. In the other part, both calculated results are almost the same.

IV. TRANSVERSE ENERGY DISTRIBUTION

What we did in Section 3 is also suitable for the investigation of the transverse energy distribution. We assume that the transverse energy ($E_{T,i}$) distribution contributed by the i -th nucleon in the projectile and target participants is

$$f_{E_T}(E_{T,i}) = \frac{1}{\langle E_{T,i} \rangle} \exp\left(-\frac{E_{T,i}}{\langle E_{T,i} \rangle}\right), \quad (12)$$

where

$$\langle E_{T,i} \rangle = \int E_{T,i} f_{E_T}(E_{T,i}) dE_{T,i} \quad (13)$$

is the mean value of the transverse energy contributed by the i -th nucleon. Then the transverse energy (E_T) distribution at a fixed b is obtained from

$$\frac{d\sigma}{dE_T(b)} = \sigma \int \prod_{i=1}^n f_{E_T}(E_{T,i}) \delta\left[\left(\sum_{i=1}^n E_{T,i}\right) - E_T\right] \prod_{i=1}^n dE_{T,i} = \frac{\sigma E_T^{n-1}}{(n-1)! \langle E_{T,i} \rangle^n} \exp\left(-\frac{E_T}{\langle E_{T,i} \rangle}\right). \quad (14)$$

The transverse energy distribution in the final state is

$$\frac{d\sigma}{dE_T} = \frac{2}{(R_P + R_T)^2} \int_0^{R_P + R_T} \frac{d\sigma}{dE_T(b)} db. \quad (15)$$

In the calculation of the transverse energy distribution in this paper, we use the Monte Carlo method. The transverse energy contributed by the i -th nucleon is given by

$$E_{T,i} = -\langle E_{T,i} \rangle \ln R_i(1). \quad (16)$$

At a fixed impact parameter b , the transverse energy is regarded as

$$E_T = -\sum_{i=1}^n \langle E_{T,i} \rangle \ln R_i(1). \quad (17)$$

The transverse energy is finally obtained by the statistical method.

The neutral transverse energy distribution in Pb-Pb collisions at 158A GeV is presented in Fig. 5. The circles are the experimental data quoted in Ref. [8] and the neutral particles with $1.1 < \eta < 2.3$. The thin continuous and dashed curves around the data are our calculated results, corresponding to the Woods-Saxon shape and even nucleon number density distribution, respectively. One can see that a difference between the calculated results and the data exists in the region of $E_T < 20$ GeV. In order to improve the calculated results, we have to increase $d\sigma/dE_T$ to $d\sigma/dE_T + 200E_T^{-3}$ in the region of $E_T < 20$ GeV for the events with $n < 20$. The improved calculated results are given in Fig. 5 by the thick continuous and dotted curves, which correspond to the Woods-Saxon shape and even

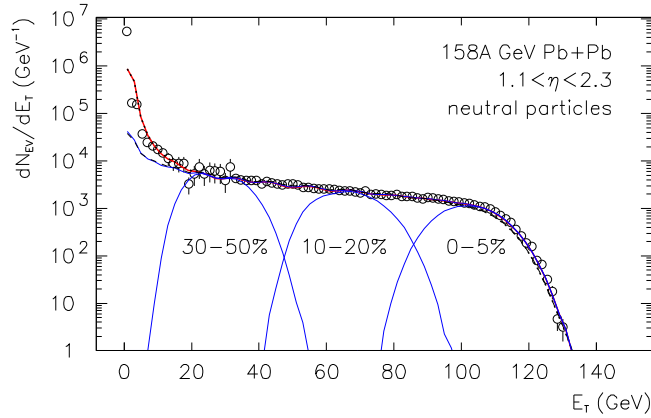


FIG. 5: Neutral transverse energy distribution in Pb-Pb collisions at 158A GeV. The circles are the experimental data quoted in Ref. [8] and the curves are our calculated results.

nucleon number density distribution, respectively. The three thin curves are our calculated results for three different centrality cuts. In the calculation, we take $\langle E_{T,i} \rangle = 0.275$ GeV. The improved calculated results corresponding to both the nucleon number density distributions are in agreement with the experimental data. For both improved calculated results, there is a little difference in the knee part. In the other part, both improved calculated results are almost the same.

V. DISCUSSIONS AND CONCLUSIONS

The parameter $\langle N_i \rangle$ is related to the cut condition. For Au-Au collisions at $\sqrt{s} = 130A$ GeV (Fig. 2), the cut condition is the negatives with $p_T > 100$ MeV/c and $|\eta| < 0.5$. For Pb-Pb collisions at 158A GeV (Figs. 3 or 4), the cut condition is the charged particles with $2.35 < \eta < 3.75$ or the γ -like clusters with $2.8 < \eta < 4.4$. It is obvious that the cut condition for the Au-Au collisions is tighter than that for the Pb-Pb collisions. This means that the parameter $\langle N_i \rangle$ has a small value in the case of the Au-Au collisions. As the basic multiplicity distribution, Eq. (6) is normalized to 1 for the i -th nucleon in the projectile and target participants. In our calculation, we have taken the parameter $\langle N_i \rangle$ to be not related to i .

It seems that a uniform distribution over the impact parameter is assumed. In fact, the distributions for different impact parameters are different due to different n . As the fold of n exponential distributions, the Erlang distribution in Eq. (8) has really different forms in the case of different impact parameters (or different n). As the first approximation, the values of $\langle N_i \rangle$ (or $\langle E_{T,i} \rangle$) for different b have been taken as the same, for a given interacting system and cut condition.

In the calculation of the multiplicity and the transverse energy distributions, we have

regarded the i -th nucleon as an energy source emitting particles. The multiplicity or transverse energy distribution for an energy source can be regarded as an exponential distribution [9]. The special form of fluctuations in Eq. (10) [or (16)] is the Monte Carlo simulation formula of an exponential distribution. If we use the typical Gaussian fluctuation, e.g. $N_i = \langle N_i \rangle + \sigma_i \sqrt{-2 \ln R_i(1)} \cos[2\pi R_i(2)]$, where σ_i and $R_i(2)$ denote the distribution width and a random variable in $[0,1]$, respectively, the calculated results can fit the tail part of the concerned experimental distribution, but cannot fit the low and middle multiplicity (or transverse energy) regions.

We investigated the emissions of nuclear fragments [10] and relativistic singly charged particles [11] in our recent work [10,11]. In the geometric picture, the relativistic and non-relativistic nuclear fragments with charge ≥ 2 are produced in the projectile and target spectators, respectively. The relativistic non-proton singly charged particles are produced in the participant, and the relativistic protons are produced in both the participant and projectile spectator. The singly charged particles with non-relativistic energy are produced in both the participant and target spectator regions in the case of intranuclear cascade collisions, or produced in the target spectator in the case of evaporation. The particles concerned in the present work are mainly relativistic singly charged or neutral particles. They are produced in the participant.

Nuclear geometry plays an important role not only in the fixed target experiment but also in the collider experiment. The multiplicity and transverse energy distributions in nucleus-nucleus collisions at the CERN-SPS and BNL-RHIC energies can be described by the consideration of nuclear geometry. In the calculation, one parameter $\langle N_i \rangle$ or $\langle E_{T,i} \rangle$ is used for the normalized multiplicity or transverse energy distribution. For the Woods-Saxon shape and even nucleon number density distribution, there is a little difference in the knee part of the calculated results. In the other part, both calculated results are almost the same. We hope to study the multiplicity and transverse energy distributions at the Large Hadron Collider (LHC) energy (about 11.4 TeV) in the near future.

Acknowledgments

This work was supported by the National Natural Science Foundation of China Grant No. 10275042, the Shanxi Scholarship Council of China Grant No. JLGB(2002)8-20021042, the Shanxi Provincial Foundation for Returned Overseas Scholars Grant No. JLGB(2001)15, the Shanxi Provincial Foundation for Natural Sciences Grant No. 20021006, and the Shanxi Provincial Foundation for Key Subjects Grant No. JJJC(2002)4.

References

- * Also at the China Center of Advanced Science and Technology (CCAST - World Laboratory), Box 8730, Beijing 100080, China; Electronic address: liufh@dns.sxtu.edu.cn
- [1] G. Odyniec, nucl-ex/0110012, Int. J. Mod. Phys. A **17**, 3107 (2002).

- [2] S. Das Gupta *et al.*, *Adv. Nucl. Phys.* **26**, 89 (2001).
- [3] J. P. Bondorf *et al.*, *Phys. Rep.* **257**, 133 (1995).
- [4] R. J. Glauber, in *Lectures of Theoretical Physics*, edited by W. E. Brittin and L. G. Dungam (Interscience, New York 1959), Vol. 1, p. 315.
- [5] A. Bialas, M. Bleszynski, and W. Czyz, *Nucl. Phys.* **B111**, 461 (1976).
- [6] STAR Collaboration, C. Adler *et al.*, nucl-ex/0106004; M. Calderón de la Barca Sánchez for the STAR Collaboration, nucl-ex/0108012.
- [7] P. Steinberg for the WA98 Collaboration, *Nucl. Phys. B (Proc. Suppl.)* **71**, 335 (1990).
- [8] NA50 Collaboration, M. C. Abreu *et al.*, CERN-EP/2002-017, *Phys. Lett. B* **530**, 33 (2002).
- [9] L. S. Liu and T. C. Meng, *Phys. Rev. D* **27**, 2640 (1983); K. C. Chou, L. S. Liu, and T. C. Meng, *Phys. Rev. D* **28**, 1080 (1983).
- [10] F. H. Liu, *Chin. J. Phys.* **40**, 159 (2002); F. H. Liu, *Chin. J. Phys.* **39**, 401 (2001); F. H. Liu, *Chin. J. Phys.* **38**, 1063 (2000).
- [11] F. H. Liu, *Chin. J. Phys.* **39**, 248 (2001); F. H. Liu, *Chin. J. Phys.* **39**, 163 (2001); F. H. Liu, *Chin. J. Phys.* **38**, 907 (2000); F. H. Liu, *Chin. J. Phys.* **38**, 42 (2000).